

# Weak 21<sup>st</sup>-century AMOC response to Greenland meltwater in a strongly eddying ocean model

Oliver Mehling and Henk A. Dijkstra

Institute for Marine and Atmospheric research Utrecht, Department of Physics, Utrecht University,  
Utrecht, The Netherlands

## Key Points:

- The impact of increasing Greenland meltwater on the AMOC under climate change is studied with a strongly eddying ocean model
- Meltwater induces an additional AMOC weakening of  $0.6 \pm 0.2$  Sv by 2100, similar to values obtained at low resolution and in coupled models
- Increasing stratification under global warming shapes the state-dependent AMOC response to Greenland meltwater

---

Corresponding author: Oliver Mehling, [o.m.mehling@uu.nl](mailto:o.m.mehling@uu.nl)

## Abstract

Climate models project that the Atlantic Meridional Overturning Circulation (AMOC) will weaken in the 21<sup>st</sup> century, but the magnitude is highly uncertain. Some of this uncertainty is structural, as most climate models neglect increasing meltwater from the Greenland ice sheet and do not explicitly capture mesoscale ocean eddies. Here, we quantify the impact of Greenland meltwater on the AMOC until 2100 under SSP5-8.5 forcing for the first time in a strongly eddying (1/10° horizontal resolution) ocean model. The meltwater-induced additional AMOC weakening is small ( $0.6 \pm 0.2$  Sv) compared to the weakening due to warming alone, and similar at high and low resolution. The same meltwater would cause a stronger AMOC weakening under present-day climate conditions. We link both resolution-independence and state-dependence to large-scale controls of the AMOC. Our results demonstrate that the background ocean state is more important than resolution in determining how Greenland meltwater affects the AMOC.

## Plain Language Summary

Human-caused global warming is expected to cause a weakening of the Atlantic Meridional Overturning Circulation (AMOC) and increased melt of the Greenland ice sheet. However, most current climate models do not represent the interaction between these two systems. The question of how strongly Greenland melt will impact the AMOC in the 21<sup>st</sup> century has already been studied in climate models with an ocean resolution of around 100 km. However, this is too coarse to explicitly capture mesoscale eddies, which could influence how meltwater propagates in the North Atlantic and how it affects the AMOC. Here, we quantify the impacts of Greenland meltwater on the AMOC until 2100 in a high-resolution (around 10 km horizontal resolution) eddy-rich ocean model. We find that the AMOC response to Greenland meltwater under global warming is similar at high and low resolution, and – consistently with previous studies – that it is small compared to the AMOC weakening driven by global warming alone. The same amount of meltwater also weakens the AMOC less strongly under global warming than under present-day climate conditions. This shows that the background ocean state is more important than resolution in determining how Greenland melt affects the AMOC.

## 1 Introduction

The Atlantic Meridional Overturning Circulation (AMOC) is expected to play an important role in shaping the climate response to future anthropogenic greenhouse gas emissions (Liu et al., 2020; Bellomo et al., 2021; Bellomo & Mehling, 2024). While there is high confidence in climate model projections that the AMOC will weaken in the 21<sup>st</sup> century (Weijer et al., 2020), the magnitude of this weakening is highly uncertain (Fox-Kemper et al., 2021). This is not only due to large inter-model spread in the simulated AMOC decline (Gregory et al., 2005; Reintges et al., 2017; Weijer et al., 2020; Bonan et al., 2025), but also due to the potential of nonlinear AMOC changes such as an abrupt AMOC collapse or tipping, the probability of which remains poorly quantified in climate models (Dijkstra & van Westen, 2026; Loriani et al., 2025).

Based on evidence from current-generation climate models, the IPCC Sixth Assessment Report assessed with “medium confidence” that the AMOC “will not experience an abrupt collapse before 2100” (Fox-Kemper et al., 2021). The main reasons for assigning only “medium confidence” to this finding were structural deficits such as model biases related to AMOC stability (Liu et al., 2017; Mecking et al., 2017; van Westen & Dijkstra, 2024) and neglected meltwater influx from the Greenland Ice Sheet (GrIS).

The impact of realistic Greenland meltwater input on 21<sup>st</sup>-century AMOC changes has been extensively studied in IPCC-class climate models with a typical ocean resolution of around 1° (e.g., Lenaerts et al., 2015; Bakker et al., 2016; Ackermann et al., 2020; Mehling et al., 2025). These models show a moderate response of less than or around 1 Sv (1 Sv =  $10^6 \text{ m}^3 \text{ s}^{-1}$ ) meltwater-induced additional AMOC weakening until 2100 but do not explicitly capture mesoscale ocean eddies. It has been shown that, under historical climate conditions, resolving mesoscale eddies can have a potentially important effect on how Greenland meltwater affects the large-scale ocean circulation (Weijer et al., 2012; Böning et al., 2016; Swingedouw et al., 2022; Martin & Biastoch, 2023; Martin-Martinez et al., 2025). While 21<sup>st</sup>-century climate projections have recently been carried out at eddy-rich (1/10° or higher) resolution (Chang et al., 2020; Jüling et al., 2021), the effect of Greenland meltwater on the AMOC under 21<sup>st</sup>-century climate change has so far not been separately assessed with an explicit representation of mesoscale eddies. To our knowledge, the only attempt in this direction has been by Li et al. (2023); how-

ever, their simulations ended in 2050, focused on the Antarctic Bottom Water response to meltwater, and did not capture any CO<sub>2</sub>-induced AMOC weakening.

In this study, we use a global ocean model at 1/10° resolution to quantify the 21<sup>st</sup>-century AMOC response to Greenland meltwater under a strong global warming scenario. A high-end but physically plausible estimate of Greenland ice sheet runoff is derived from a fully coupled climate–ice sheet model simulation (Muntjewerf et al., 2020). Comparison with the low-resolution version of the same model and a set of previous, more idealized Greenland meltwater simulations under present-day conditions (Weijer et al., 2012) allow disentangling the impacts of resolution and background climate state on the AMOC response to 21<sup>st</sup>-century Greenland melt.

## 2 Materials and Methods

### 2.1 Global ocean model

Simulations are performed with version 2 $\alpha$  of the Parallel Ocean Program (POP; Dukowicz & Smith, 1994). The high-resolution global configuration of POP (Maltrud et al., 2010; Weijer et al., 2012) (HR-POP hereafter) has a resolution of 1/10° using a tripolar grid in the horizontal and 42 levels in the vertical, with a top-layer thickness of 10 m. This configuration has been extensively used in previous studies related to AMOC stability (Weijer et al., 2012; den Toom et al., 2014; Brunnabend & Dijkstra, 2017; van Westen et al., 2025) and has been shown to be in reasonable agreement with observations in the subpolar North Atlantic (Weijer et al., 2012; Fried et al., 2024). The model is forced by reanalysis-derived heat and freshwater fluxes and wind stress (Large & Yeager, 2004) described in more detail in Text S1 of the Supplementary Information. This version of POP does not include interactive sea ice, and instead salinity is restored with a timescale of 30 days under a prescribed seasonal sea ice extent. No salinity restoring is applied elsewhere.

For comparison, we also use the low-resolution (1°) version of POP (LR-POP hereafter), which has been configured to closely match the HR-POP control state (see Supplementary Information of Weijer et al. (2012) for a detailed description and validation of both). At this ocean resolution, which is typical for current-generation coupled climate models, the effects of mesoscale eddies on tracer transport are parameterized (Gent & McWilliams, 1990) instead of explicitly captured. LR-POP uses a dipole grid with the

North Pole over Greenland with 40 vertical levels. The resolution of LR-POP reaches around 50 km in the Labrador Sea, compared to around 6 km in HR-POP.

## 2.2 Experiment setup

We probe the impact of Greenland meltwater in the 21<sup>st</sup> century under the SSP5-8.5 scenario (O'Neill et al., 2016), the strongest global warming scenario considered in the Coupled Model Intercomparison Project phase 6 (CMIP6; Eyring et al., 2016). As described in Text S1 of the Supplementary Information, we derive the surface boundary conditions for ocean-only future projections from CMIP6 multi-model mean anomalies of all forcing fields except runoff. These anomalies are referenced to the 1958–2000 climatology because the POP control run was integrated using fixed “normal-year” forcing (Large & Yeager, 2004) representative of the 1958–2000 period. To avoid spurious breaks between historical and future forcing, we use the CMIP6 multi-model mean anomalies for both. The seasonal cycle is taken into account for all forcing anomalies, but year-to-year variations are smoothed with a 20-year running mean to isolate long-term changes and for consistency with the control run, which also has no forced interannual variability.

The historical + SSP5-8.5 (“Reference”) simulation is branched off from year 170 of an existing HR-POP control run (Le Bars et al., 2016). The branching point is defined as year 1978, where the global mean CMIP6-derived anomalies are closest to zero. A second simulation (“Meltwater”) is branched off from the “Reference” simulation in 2000 with the same forcing anomalies, but with added Greenland meltwater from the fully coupled climate–ice sheet model CESM2-CISM2 (Muntjewerf et al., 2020). The meltwater forcing is described in more detail in Text S2 of the Supplementary Information and in Mehling et al. (2025), who applied the same meltwater forcing in a coupled climate model. Greenland runoff is aggregated into seven drainage basins (Mouginot et al., 2019) before being inserted in the uppermost model layer in a radius of around 30 km of the coast (Supplementary Fig. S1). The total Greenland runoff anomaly reaches around 0.09 Sv in 2100.

To assess the sensitivity of our results to horizontal resolution, we perform the same set of experiments with LR-POP at 1° resolution. In addition, we test the state-dependence of Greenland meltwater impacts on the AMOC by adding the same time-dependent Green-

land meltwater input as in the future projections but with the fixed “normal-year” forcing, mentioned earlier. Due to the extreme computational cost of HR-POP (nearly 10,000 CPU hours per model year), this experiment could only be performed with LR-POP. However, a set of more idealized experiments with HR-POP, in which a constant 0.1 Sv runoff was inserted around Greenland with a similar geographical distribution under normal-year forcing, is available from [Weijer et al. \(2012\)](#). The cumulative meltwater input in the “Meltwater” simulations until 2100 is 2.5 Sv year, a value reached after 25 years in the “0.1 Sv” simulations. Therefore, we compare their AMOC anomalies after 25 years (subtracting AMOC changes in the control run during the same period) to add robustness to our analysis of state-dependence.

### 2.3 AMOC analysis

The AMOC strength in the model simulations is first computed from the annual mean overturning streamfunction in depth coordinates by identifying the streamfunction maximum below 500 m at 26.5°N. To identify drivers of AMOC changes, we relate the Atlantic overturning to the vertical structure of the meridional density gradient via the thermal wind balance relation, an approach which has already been successfully applied across different general circulation models ([de Boer et al., 2010](#); [Butler et al., 2016](#); [Haskins et al., 2019](#); [Bonan et al., 2022](#); [Nayak et al., 2024](#); [Bonan et al., 2025](#); [Vanderborght et al., 2025](#); [Mehling et al., 2026](#)). Specifically, [Bonan et al. \(2025\)](#) showed that 21<sup>st</sup>-century AMOC weakening can be reconstructed across different CMIP6 models and scenarios using the relation

$$\Psi = C \frac{g}{\rho_0 f} \langle \Delta_y \rho \rangle H^2, \quad (1)$$

where  $\Psi$  is the AMOC strength (here defined as the maximum below 500 m and between the equator and 30°N),  $\langle \Delta_y \rho \rangle$  is the vertically integrated density difference between the North and the South Atlantic,  $H$  is the scale (or pycnocline) depth defined below,  $g = 9.81 \text{ m s}^{-2}$  is the gravitational acceleration,  $\rho_0 = 1026 \text{ kg m}^{-3}$  is the seawater density,  $f = 10^{-4}$  is the Coriolis parameter at mid-latitudes, and  $C$  is a proportionality constant that relates the zonal to the meridional density gradient (e.g., [Marotzke, 1997](#); [Vanderborght et al., 2025](#)). [Bonan et al. \(2025\)](#) used  $C = 0.5$  but the value of  $C$  is poorly constrained by theory (e.g., [Gnanadesikan, 1999](#); [Mehling et al., 2026](#)). Instead, as in [Vanderborght et al. \(2025\)](#) and [Mehling et al. \(2026\)](#), we treat  $C$  as a free parameter that is obtained by regressing the anomalies of the right-hand side of Eq. (1) onto the mod-

eled AMOC anomaly for the “Reference” experiment, separately for the high- and low-resolution versions.

Following [Bonan et al. \(2025\)](#), the density gradient  $\Delta_y\rho$  is defined as the difference between the vertically averaged potential density over the upper 2000 m between a box in the North Atlantic (43°N–65°N) and the South Atlantic (30°S–30°N). Here, the best reconstruction is achieved when the potential density is referenced to 2000 m for HR-POP and to the surface for LR-POP. Our conclusions remain unchanged when referencing potential density to 2000 m in both configurations (as in [Bonan et al. \(2025\)](#)), but the residual would increase for LR-POP especially under “normal-year” forcing. Finally, the scale depth is defined as the depth  $H$  where the depth-integrated density gradient is equal to the vertical mean of the depth-integrated density gradient (Eq. 8 of [de Boer et al., 2010](#)):

$$\int_H^0 \Delta_y\rho(z) dz = \frac{1}{D} \int_D^0 \int_z^0 \Delta_y\rho(z') dz' dz. \quad (2)$$

### 3 Results

#### 3.1 AMOC response to Greenland meltwater across resolutions and climate states

AMOC timeseries at 26.5°N are shown in Fig. 1a for the high-resolution POP experiments. The present-day (2004–2022) AMOC strength at this latitude compares favorably to the around 17 Sv observed at the RAPID array ([Johns et al., 2023](#)). As expected, the AMOC weakens in the future projections due to the strong CO<sub>2</sub>-induced climate change forcing. By the end of the century (2090–2100), the AMOC decrease compared to the present-day observational period is 9.7 Sv, which is towards the upper end of the range of AMOC weakening simulated by CMIP6 models ([Weijer et al., 2020](#)). However, both the initial and the end-of-the-century AMOC states fall well within the CMIP6 range. The relatively monotonic AMOC weakening appears to be superimposed by intrinsic multi-decadal variability, which has previously been described in the control simulation ([Le Bars et al., 2016](#)).

The effect of Greenland meltwater, i.e., the difference between the AMOC strength in the “Meltwater” and “Reference” simulations, is relatively small throughout the 21<sup>st</sup> century. The mean difference over 2080–2100 is only  $0.6 \pm 0.2$  Sv but statistically significant ( $p = 0.003$  using a Student’s *t*-test). The effect is very similar in LR-POP ( $0.5 \pm 0.1$  Sv,

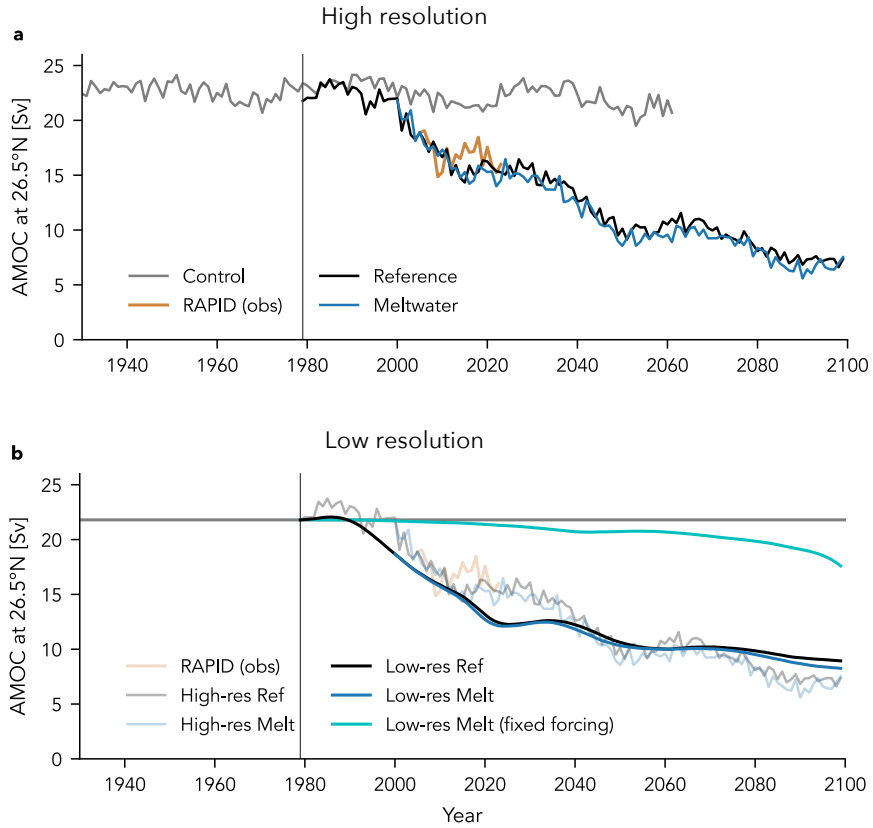


**Figure 1. AMOC timeseries at  $26.5^{\circ}\text{N}$  under historical and SSP5-8.5 forcing in the (a) high-resolution ( $1/10^{\circ}$ ) POP and (b) low-resolution ( $1^{\circ}$ ) POP. Black lines are the “Reference” simulations with climate change forcing only and blue lines are the “Meltwater” simulations with climate change and Greenland meltwater forcing. The cyan line in panel b is with Greenland meltwater forcing only and otherwise fixed climate boundary conditions. The observed (2004–2024) AMOC time series from the RAPID array (Moat et al., 2025) is also shown in panel a. For comparison, the main results from the high-resolution simulation are duplicated semi-transparently in panel b.**

$p < 0.001$ ), although the remaining AMOC is slightly stronger at low resolution (8.8 Sv vs. 6.9 Sv with Greenland meltwater, Fig. 1b).

The meltwater effect on the AMOC in HR-POP is consistent across the Atlantic basin. When calculating the AMOC in density space, the largest meltwater-induced AMOC weakening at the end of the 21<sup>st</sup> century can be found in the subpolar North Atlantic between 50°N to 70°N (Supplementary Fig. S2). This is unsurprising given that most of the Greenland runoff enters the Atlantic around these latitudes, but points towards a potentially earlier detection of a robust meltwater signal in the AMOC at the OSNAP observational array in the subpolar North Atlantic (Lozier et al., 2019) compared to RAPID at 26°N.

While the difference in meltwater-induced AMOC weakening between the high- and low-resolution versions is very small, important differences arise in the low-resolution POP when the same time-dependent Greenland meltwater input is inserted under fixed normal-year forcing instead of 21<sup>st</sup>-century climate change (cyan line in Fig. 1b). Under fixed normal-year (i.e., 20th-century) forcing, the AMOC weakens by more than 3 Sv, yielding a six-fold stronger Greenland meltwater effect on the AMOC than under transient 21<sup>st</sup>-century forcing. For comparison, in the 0.1 Sv Greenland hosing experiments of Weijer et al. (2012), the AMOC weakened similarly by about 4 Sv and 4.5 Sv after 25 years in LR-POP and HR-POP, respectively. This indicates that the state-dependence of Greenland meltwater on the AMOC appears robust across resolutions.

### 3.2 Meltwater propagation pathways

The propagation of Greenland meltwater can be compared across resolutions and background climate states using a passive freshwater tracer (cf. Böning et al., 2016; Martin et al., 2022), which follows the same model physics as the prognostic salinity. Maps of tracer concentrations by depth at the end of the 21<sup>st</sup> century are shown in the Supplementary Material (Supplementary Fig. S3). Except for the region of meltwater input, the highest concentrations of the meltwater tracer can be found near the surface in Baffin Bay and along the Labrador Current at both resolutions. In contrast, again at both high and low resolution, much less meltwater reaches the interior of the subpolar gyre, with higher concentrations in the subtropical gyre. The main differences between resolutions are that more meltwater remains around the Grand Banks or along North

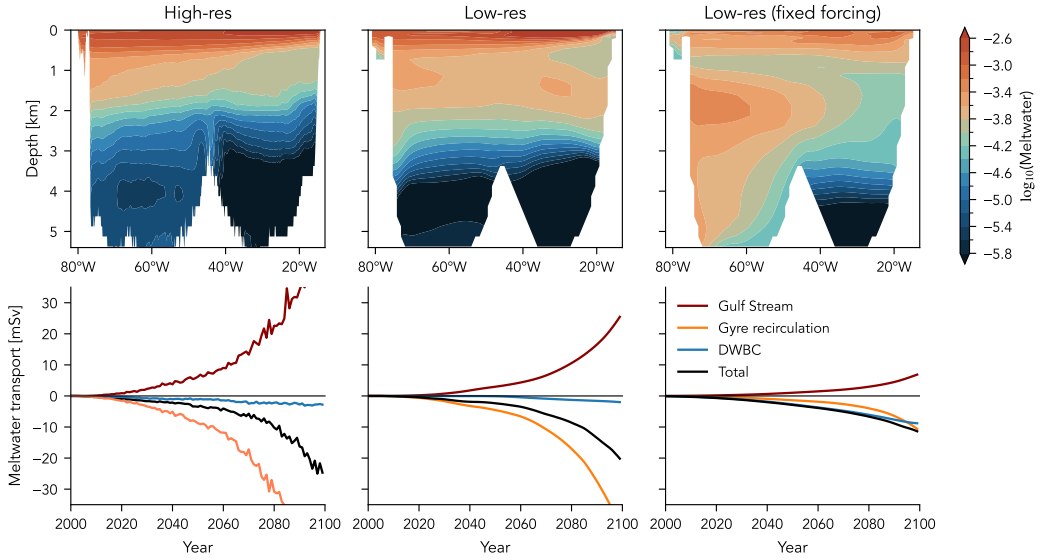


**Figure 2. Meltwater tracer concentration and transport at 26°N:** (a-c) Concentration of the meltwater tracer (on a logarithmic scale) in the year 2100, (d-f) Meltwater transport across 26°N (black) decomposed into transport by the Gulf Stream, transport in the upper 1000 m excluding the Gulf Stream (“gyre recirculation”), and by the deep western boundary current (DWBC). The transport below 1000 m outside of the DWBC is very small and not shown.

American East coast at high resolution, and that more meltwater reaches subtropical gyre, especially below 200m. Both these differences were also found by [Martin and Biastoch \(2023\)](#) with a different ocean model under historical forcing but also had little effect on the AMOC weakening.

To relate the meltwater propagation pathways to the AMOC, we analyze a cross-section at 26°N (Fig. 2) where the meridional velocity that underlies the AMOC calculation can be decomposed into components from the Gulf Stream, the deep western boundary current (DWBC), and recirculation within by the subtropical gyre ([Asbjørnsen & Árthun, 2023](#)). Following the methodology detailed in [Asbjørnsen and Árthun \(2023\)](#), the cores of the (northward, upper-ocean) Florida and Antilles Currents, which add up to the Gulf Stream transport, as well as of the (southward, deep-ocean) DWBC are identified in the meridional velocity cross-sections. Tracer transports are then calculated by masking these cores, and the residual transport over the upper 1000 m is defined as the subtropical gyre recirculation. At the end of the 21<sup>st</sup> century, most of the net (southward) meltwater transport can be attributed to the upper 1000 m, with both a large re-

circulation within the subpolar gyre and a southward transport mostly along the Eastern boundary. In contrast, the DWBC only accounts for around 10% of the net meltwater transport. This fundamentally differs from the simulation under fixed normal-year forcing, where the net meltwater transport is almost identical to the meltwater transport by the DWBC, and the gyre recirculation is also much smaller.

These differences between the two climate states can be related to the different tracer distributions (first row of Fig. 2). In the future scenario, most of the meltwater remains near the surface at both resolutions, with highest concentrations on the Eastern side of the basin. Hence, a large portion of the southward meltwater transport appears to be via the Canary Current. Under fixed forcing, tracer concentrations in the upper ocean and especially in the Eastern North Atlantic are much lower, and in turn more meltwater has reached the deep ocean below 1000 m (cf. Supplementary Fig. S3). This is especially the case in the DWBC on the western side of the basin, where meltwater tracer concentrations are more than an order of magnitude larger than in the future scenarios (Fig. 2).

### 3.3 Large-scale controls of Greenland meltwater impacts

The similar AMOC response to future Greenland meltwater input in the high- and low-resolution POP versions suggests that large-scale properties rather than (eddy-related) mesoscale features control the impacts of meltwater. One straightforward mechanism is the shallowing of deep convection under global warming, which is similar in both resolutions (Fig. 3) and linked to increasing ocean stratification (cf. [Cheng et al., 2025](#)). Winter mixed layers, which exceed 1000 m in parts of the Labrador Sea and Nordic Seas in the control simulation, become shallower than 500 m across the subpolar North Atlantic by the end of the century (Fig. 3), which provides a mechanism for why more meltwater remains confined to the upper hundreds of meters and why only very little reaches the DWBC (Fig. 2), independently of resolution.

We can also relate the AMOC response to Greenland meltwater to large-scale properties of the North Atlantic more quantitatively using the thermal wind balance framework of [Bonan et al. \(2025\)](#). Following their methodology to diagnose AMOC weakening across different future warming scenarios, we decompose AMOC changes due to global warming and/or Greenland meltwater input into a component due to changes in scale

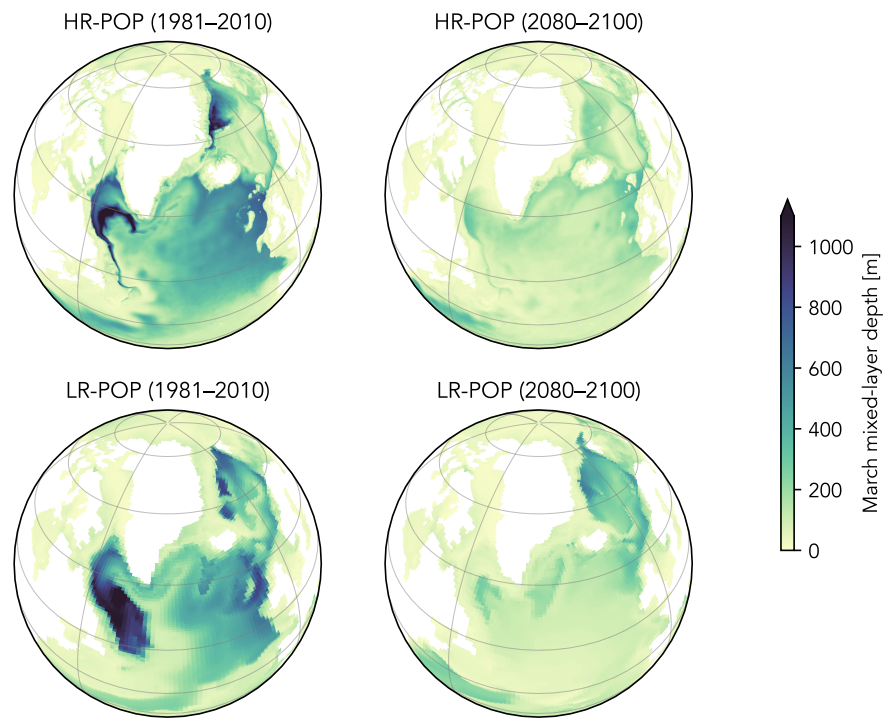


**Figure 3.** Mixed-layer depth in March for HR-POP (first row) and LR-POP (second row) for 1981–2010 (first column) and 2080–2100 (second column). For 2080–2100, mixed-layer depths are shown from the “Meltwater” simulations, but they do not differ strongly from the “Reference” simulations for the same period.

depth  $H$  and meridional density gradient  $\Delta\rho_y$ . We compare the present-day (1981–2010) AMOC to the AMOC state at the end of the 21<sup>st</sup> century (2080–2100).

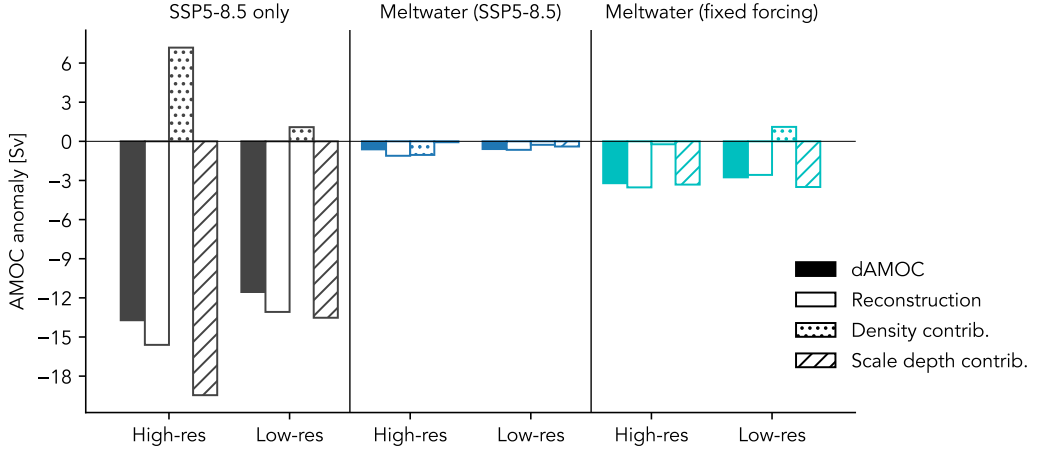


**Figure 4. AMOC changes attributed to density gradient and scale depth changes.**

For each simulation, the AMOC anomaly (filled bars) is shown along with the reconstructed AMOC anomaly from thermal wind balance (non-filled bars) and its partitioning in a density gradient ( $\Delta_y\rho$ ) and a scale depth ( $H$ ) contribution. The pairs (high and low resolution) of AMOC anomalies are color-coded as follows. AMOC weakening (2080–2100 minus 1981–2010) due to SSP5-8.5 CO<sub>2</sub> forcing only: black, AMOC anomaly due to Greenland meltwater under SSP5-8.5 forcing (2080–2100): blue, AMOC anomaly due to Greenland meltwater under fixed normal-year forcing: cyan.

As in the CMIP6 ensemble (Bonan et al., 2025), the AMOC weakening due to global warming in POP (first group in Fig. 4) is mainly driven by changes in scale depth  $H$ . The small contribution of density gradient changes in fact slightly opposes the AMOC weakening (cf. de Boer et al., 2010). Similarly, the AMOC weakening due to Greenland meltwater under fixed climate forcing (last group in Fig. 4) is mainly explained by the decreasing scale depth contribution. In contrast, under global warming, the Greenland meltwater input barely affects the (already strongly reduced) scale depth (second group in Fig. 4), and the meltwater effect is instead caused by a decrease in the meridional density gradient. This mechanism appears to be much less effective in weakening the AMOC than the scale depth changes. All these results are consistent across both resolutions.

One can also re-calculate the scale depth (Eq. 2) for HR-POP by adding the meltwater-induced density anomalies from the “0.1 Sv” fixed-forcing simulation to the density profile for 2080–2100 under SSP5-8.5 forcing without Greenland meltwater. This leads to only a slight shallowing of the scale depth from 810 m to 804 m, corresponding to an AMOC weakening of 0.3 Sv. For comparison, with a fixed background climate, the scale depth decrease induced by the same density anomaly is from 1164 m to 1126 m, corresponding to an AMOC weakening of 3.3 Sv. This calculation illustrates the dominant role of mean-state changes in the ocean density profile for the impacts of Greenland meltwater under global warming.

#### 4 Discussion and Conclusions

In this study, we presented the first estimate of the impacts of 21<sup>st</sup>-century Greenland ice sheet melt on the AMOC at eddy-resolving (1/10°) ocean model resolution. Our results showed that the meltwater impact on AMOC strength by 2100 is statistically significant but small, on the order of 0.5 Sv. This number is consistent between eddy-resolving and eddy-parameterizing (1°) ocean resolutions and is in good quantitative agreement with previous estimates from coupled models at 1° or coarser ocean resolution (Lenaerts et al., 2015; Bakker et al., 2016; Mehling et al., 2025).

The similar AMOC response at eddy-rich and eddy-parameterizing resolution may seem at odds with several studies claiming a potentially larger AMOC response to freshwater changes with explicit mesoscale eddies (Weijer et al., 2012; Swingedouw et al., 2022; Shan et al., 2024). However, Weijer et al. (2012) showed that the difference between the AMOC weakening at high and low resolution is moderate as long as the meltwater input is along the Greenland coast instead of uniformly “hosing” the North Atlantic. In most other studies, it is difficult if not impossible to discern the role of resolution from other factors such as differences in atmosphere–ocean coupling (Swingedouw et al., 2022) and different model biases at high and low resolution (Shan et al., 2024). The most comprehensive attempt to disentangle some of these factors has been by Martin and Biasch (2023), who compared the AMOC response to Greenland meltwater in high- and low-resolution configurations with and without atmosphere–ocean coupling. Our results (under global warming) confirm their finding (under fixed historical conditions) that, despite different meltwater propagation pathways, the AMOC response to Greenland runoff is similar across high- and low-resolution configurations.

To explain the physical mechanism behind the absence of a resolution-dependent AMOC response to Greenland meltwater, we applied the AMOC reconstruction method of [Bonan et al. \(2025\)](#) based on a thermal wind balance framework. This way, it was possible to relate the AMOC changes to a few large-scale metrics, in particular the scale depth  $H$ . This relation also appears to hold the key to the second main finding of our study, the robust state-dependence of the AMOC response to Greenland meltwater. We showed that the scale depth is barely affected when meltwater is added in a significantly warmer climate, while it controls the much stronger AMOC response to meltwater under constant historical climate conditions.

This aligns well with a previous multi-model study ([Swingedouw et al., 2015](#)) which explained the state-dependence (in eddy-parameterizing coupled models) by stratification changes and differences in the “Canary Current freshwater leakage” (cf. [Swingedouw et al., 2013](#)). In our simulations, there is also a significantly enhanced southward meltwater transport along the Canary Current in a warmer climate (Fig. 2). [Swingedouw et al. \(2015\)](#) linked this to a more zonally tilted boundary between the subtropical and subpolar gyres under global warming, which is also present in our simulations (Supplementary Fig. S4), but the exact mechanisms how this relates to AMOC weakening remain poorly understood and should be studied in more detail in the future.

In summary, we showed that Greenland meltwater only has a moderate impact (below 1 Sv) on the AMOC in future projections until 2100, even when explicitly representing mesoscale eddies, due to the significant state-dependence of meltwater input linked to stratification changes under global warming. The main limitation of our study is the use of a single model without atmosphere–ocean coupling. However, given that [Martin and Biastoch \(2023\)](#) reached similar conclusions regarding the resolution-dependence with a different ocean model and atmosphere–ocean coupling, we expect that our findings would hold in other (coupled) models. In fact, including atmospheric coupling would be expected to further dampen the meltwater-induced AMOC weakening ([Martin & Biastoch, 2023](#)).

The moderate impact of 21<sup>st</sup>-century Greenland melt does not preclude stronger effects on the AMOC after 2100 ([Bakker et al., 2016](#); [Mehling et al., 2025](#)) when Greenland melt would increase further under continued warming. Nevertheless, the moderate meltwater effect contrasts with the large uncertainty in the magnitude of 21<sup>st</sup>-century AMOC weakening due to CO<sub>2</sub> forcing alone ([Weijer et al., 2020](#); [Bonan et al., 2025](#)). There

are so far no indications that this uncertainty is linked to resolution (Winton et al., 2014; Jüling et al., 2021), but instead it is often attributed to different model biases in the mean-state (cf. Jackson et al., 2023). Combined with these previous studies, our results therefore imply that improving (ocean) resolution alone is not a silver bullet to improving AMOC projections and that reducing coupled model biases, which can be prohibitively expensive at high resolution, might be a more promising avenue to tackling the large uncertainty in AMOC projections.

## Open Research Section

The underlying data and Jupyter Notebooks to reproduce all figures are available on Zenodo: <https://doi.org/10.5281/zenodo.18324588> (Mehling, 2026). RAPID data were obtained from <https://rapid.ac.uk/> (Moat et al., 2025).

## Acknowledgments

We thank Michael Kliphuis for his kind assistance in setting up the POP simulations and for recovering data from Weijer et al. (2012), Elian Vanderborght for insightful discussions about the thermal wind balance framework, and Andy Hogg for valuable clarifications about the setup of Li et al. (2023).

This work was funded by the European Research Council through the ERC-AdG project TAOC (PI: Dijkstra, project 101055096). The model simulations were performed on the Dutch National Supercomputer Snellius within NWO-SURF project 2024.013.

## References

Ackermann, L., Danek, C., Gierz, P., & Lohmann, G. (2020). AMOC Recovery in a Multicentennial Scenario Using a Coupled Atmosphere-Ocean-Ice Sheet Model. *Geophys. Res. Lett.*, 47. doi: 10.1029/2019GL086810

Asbjørnsen, H., & Årthun, M. (2023). Deconstructing Future AMOC Decline at 26.5°N. *Geophys. Res. Lett.*, 50, e2023GL103515. doi: 10.1029/2023GL103515

Bakker, P., Schmittner, A., Lenaerts, J. T. M., Abe-Ouchi, A., Bi, D., van den Broeke, M. R., ... Yin, J. (2016). Fate of the Atlantic Meridional Overturning Circulation: Strong decline under continued warming and Greenland melting. *Geophys. Res. Lett.*, 43, 12,252–12,260. doi: 10.1002/2016GL070457

Bellomo, K., Angeloni, M., Corti, S., & von Hardenberg, J. (2021). Future climate change shaped by inter-model differences in Atlantic meridional overturning circulation response. *Nat. Commun.*, *12*, 3659. doi: 10.1038/s41467-021-24015-w

Bellomo, K., & Mehling, O. (2024). Impacts and State-Dependence of AMOC Weakening in a Warming Climate. *Geophys. Res. Lett.*, *51*, e2023GL107624. doi: 10.1029/2023GL107624

Bonan, D. B., Thompson, A. F., Newsom, E. R., Sun, S., & Rugenstein, M. (2022). Transient and Equilibrium Responses of the Atlantic Overturning Circulation to Warming in Coupled Climate Models: The Role of Temperature and Salinity. *J. Clim.*, *35*, 5173–5193. doi: 10.1175/JCLI-D-21-0912.1

Bonan, D. B., Thompson, A. F., Schneider, T., Zanna, L., Armour, K. C., & Sun, S. (2025). Observational constraints imply limited future Atlantic meridional overturning circulation weakening. *Nat. Geosci.*, *18*, 479–487. doi: 10.1038/s41561-025-01709-0

Böning, C. W., Behrens, E., Biastoch, A., Getzlaff, K., & Bamber, J. L. (2016). Emerging impact of Greenland meltwater on deepwater formation in the North Atlantic Ocean. *Nat. Geosci.*, *9*, 523–527. doi: 10.1038/ngeo2740

Brannabend, S.-E., & Dijkstra, H. A. (2017). Asymmetric response of the Atlantic Meridional Ocean Circulation to freshwater anomalies in a strongly-eddying global ocean model. *Tellus A*, *69*, 1299283. doi: 10.1080/16000870.2017.1299283

Butler, E. D., Oliver, K. I. C., Hirschi, J. J.-M., & Mecking, J. V. (2016). Reconstructing global overturning from meridional density gradients. *Clim. Dyn.*, *46*, 2593–2610. doi: 10.1007/s00382-015-2719-6

Chang, P., Zhang, S., Danabasoglu, G., Yeager, S. G., Fu, H., Wang, H., … Wu, L. (2020). An Unprecedented Set of High-Resolution Earth System Simulations for Understanding Multiscale Interactions in Climate Variability and Change. *J. Adv. Model. Earth Syst.*, *12*, e2020MS002298. doi: 10.1029/2020MS002298

Cheng, L., Li, G., Long, S.-M., Li, Y., Von Schuckmann, K., Trenberth, K. E., … Yuan, H. (2025). Ocean stratification in a warming climate. *Nat. Rev. Earth Environ.*, *6*, 637–655. doi: 10.1038/s43017-025-00715-5

de Boer, A. M., Gnanadesikan, A., Edwards, N. R., & Watson, A. J. (2010). Merid-

ional Density Gradients Do Not Control the Atlantic Overturning Circulation. *J. Phys. Oceanogr.*, *40*, 368–380. doi: 10.1175/2009JPO4200.1

den Toom, M., Dijkstra, H. A., Weijer, W., Hecht, M. W., Maltrud, M. E., & Van Sebille, E. (2014). Response of a Strongly Eddying Global Ocean to North Atlantic Freshwater Perturbations. *J. Phys. Oceanogr.*, *44*, 464–481. doi: 10.1175/JPO-D-12-0155.1

Dijkstra, H. A., & van Westen, R. M. (2026). The Probability of an AMOC Collapse Onset in the Twenty-First Century. *Annu. Rev. Mar. Sci.*, *18*, 23–46. doi: 10.1146/annurev-marine-040324-024822

Dukowicz, J. K., & Smith, R. D. (1994). Implicit free-surface method for the Bryan-Cox-Semtner ocean model. *J. Geophys. Res. Oceans*, *99*, 7991–8014. doi: 10.1029/93JC03455

Eyring, V., Bony, S., Meehl, G. A., Senior, C. A., Stevens, B., Stouffer, R. J., & Taylor, K. E. (2016). Overview of the Coupled Model Intercomparison Project Phase 6 (CMIP6) experimental design and organization. *Geosci. Model Dev.*, *9*, 1937–1958. doi: 10.5194/gmd-9-1937-2016

Fox-Kemper, B., Hewitt, H., Xiao, C., Adalgeirsdóttir, G., Drijfhout, S., Edwards, T., ... Yu, Y. (2021). Ocean, Cryosphere and Sea Level Change [Book Section]. In V. Masson-Delmotte et al. (Eds.), *Climate Change 2021: The Physical Science Basis. Contribution of Working Group I to the Sixth Assessment Report of the Intergovernmental Panel on Climate Change* (pp. 1211–1362). Cambridge, United Kingdom and New York, NY, USA: Cambridge University Press. doi: 10.1017/9781009157896.011

Fried, N., Katsman, C. A., & de Jong, M. F. (2024). Where do the Two Cores of the Irminger Current Come From? A Lagrangian Study Using a 1/10° Ocean Model Simulation. *J. Geophys. Res. Oceans*, *129*, e2023JC020713. doi: 10.1029/2023JC020713

Gent, P. R., & McWilliams, J. C. (1990). Isopycnal Mixing in Ocean Circulation Models. *J. Phys. Oceanogr.*, *20*, 150–155. doi: 10.1175/1520-0485(1990)020<0150:IMIOCM>2.0.CO;2

Gnanadesikan, A. (1999). A Simple Predictive Model for the Structure of the Oceanic Pycnocline. *Science*, *283*, 2077–2079. doi: 10.1126/science.283.5410.2077

Gregory, J. M., Dixon, K. W., Stouffer, R. J., Weaver, A. J., Driesschaert, E., Eby, M., ... Thorpe, R. B. (2005). A model intercomparison of changes in the Atlantic thermohaline circulation in response to increasing atmospheric CO<sub>2</sub> concentration. *Geophys. Res. Lett.*, 32. doi: 10.1029/2005GL023209

Haskins, R. K., Oliver, K. I. C., Jackson, L. C., Drijfhout, S. S., & Wood, R. A. (2019). Explaining asymmetry between weakening and recovery of the AMOC in a coupled climate model. *Clim. Dyn.*, 53, 67–79. doi: 10.1007/s00382-018-4570-z

Jackson, L. C., Hewitt, H. T., Bruciaferri, D., Calvert, D., Graham, T., Guiavarc'h, C., ... Storkey, D. (2023). Challenges simulating the AMOC in climate models. *Phil. Trans. R. Soc. A*, 381, 20220187. doi: 10.1098/rsta.2022.0187

Johns, W. E., Eliot, S., Smeed, D. A., Moat, B., King, B., Volkov, D. L., & Smith, R. H. (2023). Towards two decades of Atlantic Ocean mass and heat transports at 26.5° N. *Phil. Trans. R. Soc. A*, 381, 20220188. doi: 10.1098/rsta.2022.0188

Jüling, A., Zhang, X., Castellana, D., von der Heydt, A. S., & Dijkstra, H. A. (2021). The Atlantic's freshwater budget under climate change in the Community Earth System Model with strongly eddying oceans. *Ocean Sci.*, 17, 729–754. doi: 10.5194/os-17-729-2021

Large, W. G., & Yeager, S. G. (2004). *Diurnal to Decadal Global Forcing For Ocean and Sea-Ice Models: The Data Sets and Flux Climatologies* (NCAR Technical Note). Boulder, Colorado: National Center for Atmospheric Research.

Le Bars, D., Viebahn, J. P., & Dijkstra, H. A. (2016). A Southern Ocean mode of multidecadal variability. *Geophys. Res. Lett.*, 43, 2102–2110. doi: 10.1002/2016GL068177

Lenaarts, J. T. M., Le Bars, D., van Kampenhout, L., Vizcaino, M., Enderlin, E. M., & van den Broeke, M. R. (2015). Representing Greenland ice sheet freshwater fluxes in climate models. *Geophys. Res. Lett.*, 42, 6373–6381. doi: 10.1002/2015GL064738

Li, Q., England, M. H., Hogg, A. M., Rintoul, S. R., & Morrison, A. K. (2023). Abyssal ocean overturning slowdown and warming driven by Antarctic meltwater. *Nature*, 615, 841–847. doi: 10.1038/s41586-023-05762-w

Liu, W., Fedorov, A. V., Xie, S.-P., & Hu, S. (2020). Climate impacts of a weakened

Atlantic Meridional Overturning Circulation in a warming climate. *Sci. Adv.*, *6*, eaaz4876. doi: 10.1126/sciadv.aaz4876

Liu, W., Xie, S.-P., Liu, Z., & Zhu, J. (2017). Overlooked possibility of a collapsed Atlantic Meridional Overturning Circulation in warming climate. *Sci. Adv.*, *3*, e1601666. doi: 10.1126/sciadv.1601666

Loriani, S., Aksenov, Y., Armstrong McKay, D. I., Bala, G., Born, A., Chiessi, C. M., ... Tharammal, T. (2025). Tipping points in ocean and atmosphere circulations. *Earth Syst. Dyn.*, *16*, 1611–1653. doi: 10.5194/esd-16-1611-2025

Lozier, M. S., Li, F., Bacon, S., Bahr, F., Bower, A. S., Cunningham, S. A., ... Zhao, J. (2019). A sea change in our view of overturning in the subpolar North Atlantic. *Science*, *363*, 516–521. doi: 10.1126/science.aau6592

Maltrud, M., Bryan, F., & Peacock, S. (2010). Boundary impulse response functions in a century-long eddying global ocean simulation. *Environ. Fluid Mech.*, *10*, 275–295. doi: 10.1007/s10652-009-9154-3

Marotzke, J. (1997). Boundary Mixing and the Dynamics of Three-Dimensional Thermohaline Circulations. *J. Phys. Oceanogr.*, *27*, 1713–1728. doi: 10.1175/1520-0485(1997)027(1713:BMATDO)2.0.CO;2

Martin, T., & Biastoch, A. (2023). On the ocean's response to enhanced Greenland runoff in model experiments: Relevance of mesoscale dynamics and atmospheric coupling. *Ocean Sci.*, *19*, 141–167. doi: 10.5194/os-19-141-2023

Martin, T., Biastoch, A., Lohmann, G., Mikolajewicz, U., & Wang, X. (2022). On Timescales and Reversibility of the Ocean's Response to Enhanced Greenland Ice Sheet Melting in Comprehensive Climate Models. *Geophys. Res. Lett.*, *49*, e2021GL097114. doi: 10.1029/2021GL097114

Martin-Martinez, E., Moreno-Chamarro, E., Goldsworth, F. W., von Storch, J.-S., Arumí-Planas, C., Kuznetsova, D., ... Ortega, P. (2025). *North Atlantic response to a quasi-realistic Greenland meltwater forcing in eddy-rich EC-Earth3P-VHR hosing simulations*. EGUsphere. doi: 10.5194/egusphere-2025-5882

Mecking, J., Drijfhout, S., Jackson, L., & Andrews, M. (2017). The effect of model bias on Atlantic freshwater transport and implications for AMOC bi-stability. *Tellus A*, *69*, 1299910. doi: 10.1080/16000870.2017.1299910

Mehling, O. (2026). *Dataset for "Weak 21st-century AMOC response to Greenland*

*meltwater in a strongly eddying ocean model".* Zenodo. doi: 10.5281/zenodo.18324588

Mehling, O., Bellomo, K., Fabiano, F., Devilliers, M., Petrini, M., Corti, S., & von Hardenberg, J. (2025). *Limited impact of Greenland meltwater on abruptness and reversibility of future Atlantic overturning changes.* arXiv. doi: 10.48550/arXiv.2509.24858

Mehling, O., Vanderborght, E., & Dijkstra, H. A. (2026). *Critical freshwater forcing for AMOC tipping in climate models – compensation matters.* EGUsphere. doi: 10.5194/egusphere-2025-6215

Moat, B., Smeed, D., Rayner, D., Johns, W., Smith, R., Volkov, D., ... Collins, J. (2025). *Atlantic meridional overturning circulation observed by the RAPID-MOCHA-WBTS (RAPID-Meridional Overturning Circulation and Heatflux Array-Western Boundary Time Series) array at 26N from 2004 to 2024 (v2024.1).* NERC EDS British Oceanographic Data Centre NOC. doi: 10.5285/3f24651e-2d44-dee3-e063-7086abc0395e

Mouginot, J., Rignot, E., Bjørk, A. A., van den Broeke, M., Millan, R., Morlighem, M., ... Wood, M. (2019). Forty-six years of Greenland Ice Sheet mass balance from 1972 to 2018. *Proc. Natl. Acad. Sci.*, 116, 9239–9244. doi: 10.1073/pnas.1904242116

Muntjewerf, L., Petrini, M., Vizcaino, M., Ernani da Silva, C., Sellevold, R., Scherrenberg, M. D. W., ... Lofverstrom, M. (2020). Greenland Ice Sheet Contribution to 21st Century Sea Level Rise as Simulated by the Coupled CESM2.1-CISM2.1. *Geophys. Res. Lett.*, 47, e2019GL086836. doi: 10.1029/2019GL086836

Nayak, M. S., Bonan, D. B., Newsom, E. R., & Thompson, A. F. (2024). Controls on the Strength and Structure of the Atlantic Meridional Overturning Circulation in Climate Models. *Geophys. Res. Lett.*, 51, e2024GL109055. doi: 10.1029/2024GL109055

O'Neill, B. C., Tebaldi, C., van Vuuren, D. P., Eyring, V., Friedlingstein, P., Hurtt, G., ... Sanderson, B. M. (2016). The Scenario Model Intercomparison Project (ScenarioMIP) for CMIP6. *Geosci. Model Dev.*, 9, 3461–3482. doi: 10.5194/gmd-9-3461-2016

Reintges, A., Martin, T., Latif, M., & Keenlyside, N. S. (2017). Uncertainty in

twenty-first century projections of the Atlantic Meridional Overturning Circulation in CMIP3 and CMIP5 models. *Clim. Dyn.*, 49, 1495–1511. doi: 10.1007/s00382-016-3180-x

Shan, X., Sun, S., Wu, L., & Spall, M. (2024). Role of the Labrador Current in the Atlantic Meridional Overturning Circulation response to greenhouse warming. *Nat. Commun.*, 15, 7361. doi: 10.1038/s41467-024-51449-9

Swingedouw, D., Houssais, M.-N., Herbaut, C., Blaizot, A.-C., Devilliers, M., & Deshayes, J. (2022). AMOC Recent and Future Trends: A Crucial Role for Oceanic Resolution and Greenland Melting? *Front. Clim.*, 4, 838310. doi: 10.3389/fclim.2022.838310

Swingedouw, D., Rodehacke, C. B., Behrens, E., Menary, M., Olsen, S. M., Gao, Y., ... Biastoch, A. (2013). Decadal fingerprints of freshwater discharge around Greenland in a multi-model ensemble. *Clim. Dyn.*, 41, 695–720. doi: 10.1007/s00382-012-1479-9

Swingedouw, D., Rodehacke, C. B., Olsen, S. M., Menary, M., Gao, Y., Mikolajewicz, U., & Mignot, J. (2015). On the reduced sensitivity of the Atlantic overturning to Greenland ice sheet melting in projections: A multi-model assessment. *Clim. Dyn.*, 44, 3261–3279. doi: 10.1007/s00382-014-2270-x

van Westen, R. M., & Dijkstra, H. A. (2024). Persistent climate model biases in the Atlantic Ocean's freshwater transport. *Ocean Sci.*, 20, 549–567. doi: 10.5194/os-20-549-2024

van Westen, R. M., Kliphus, M., & Dijkstra, H. A. (2025). Collapse of the Atlantic Meridional Overturning Circulation in a Strongly Eddying Ocean-Only Model. *Geophys. Res. Lett.*, 52, e2024GL114532. doi: 10.1029/2024GL114532

Vanderborght, E., van Westen, R. M., & Dijkstra, H. A. (2025). Feedback Processes causing an AMOC Collapse in the Community Earth System Model. *J. Clim.*, 38, 5083–5102. doi: 10.1175/JCLI-D-24-0570.1

Weijer, W., Cheng, W., Garuba, O. A., Hu, A., & Nadiga, B. T. (2020). CMIP6 Models Predict Significant 21st Century Decline of the Atlantic Meridional Overturning Circulation. *Geophys. Res. Lett.*, 47, e2019GL086075. doi: 10.1029/2019GL086075

Weijer, W., Maltrud, M. E., Hecht, M. W., Dijkstra, H. A., & Kliphus, M. A. (2012). Response of the Atlantic Ocean circulation to Greenland Ice Sheet

melting in a strongly-eddying ocean model. *Geophys. Res. Lett.*, 39. doi:  
10.1029/2012GL051611

Winton, M., Anderson, W. G., Delworth, T. L., Griffies, S. M., Hurlin, W. J.,  
& Rosati, A. (2014). Has coarse ocean resolution biased simulations of  
transient climate sensitivity? *Geophys. Res. Lett.*, 41, 8522–8529. doi:  
10.1002/2014GL061523